ELSEVIER

Journal of Nuclear Materials 264 (1999) 122–132

journal of nuclear materials

Isotope selective excitation of ^{155}Gd and ^{157}Gd isotopes from $^{9}D^{\circ}_{2-6}$ states using broadband lasers

M. Sankari *, M.V. Suryanarayana, S. Gangadharan

National Centre for Compositional Characterisation of Materials ECIL (PO), Hyderabad 500 062, India

Received 29 April 1998; accepted 1 July 1998

Abstract

The feasibility of isotope enrichment of ^{155}Gd and ^{157}Gd isotopes using relatively broadband lasers within the tuning range of rhodamine-6G dye has been studied. A new set of photoionization schemes have been proposed for using in the industrial scale enrichment of these isotopes. These photoionization schemes result in better photon economy compared to the photoionization schemes reported earlier. The enriched isotopic mixture results in a 50% increase in the neutron absorption cross-section and a 70% reduction in the residual neutron absorption. The degree of enrichment of the odd isotopes is adequate for using the enriched mixture as an efficient burnable poison. The effect of linewidth of the excitation laser and Doppler width of the atom source on the degree of enrichment have been theoretically evaluated and experimentally verified. The computed selectivities were in good agreement with the experimental results.

1. Introduction

Gadolinium has seven naturally occurring isotopes ^{152}Gd (0.20%), ^{154}Gd (2.15%), ^{155}Gd (14.73%), ^{156}Gd (20.47%), ^{157}Gd (15.68%), ^{158}Gd (24.87%) and ^{160}Gd (21.90%). Gadolinium is extensively being used as burnable poison [1,2] in nuclear reactors because, the odd isotopes ^{155}Gd and ^{157}Gd have extremely large thermal neutron absorption cross-sections of 60,900 and 254,000 b respectively. An ideal burnable poison should be a strong neutron absorber and its daughter product of the (n, γ) reaction should have negligibly small neutron absorption cross-section. However, the low abundant ^{152}Gd and ^{154}Gd isotopes in spite of having sizable thermal neutron absorption cross-section (735 and 85 b respectively), do not burn completely. Moreover, ^{152}Gd isotope produces ^{153}Gd isotope which has significant thermal neutron absorption cross-section (36,000 b). This results in large residual absorption in the irradiated fuel. Hence, in order to use gadolinium as an efficient burnable poison, it should be enriched in odd isotopes as well as depleted in ^{152}Gd and ^{154}Gd isotopes. This ensures significant reduction in the volume of the burnable poison. The other even isotopes ^{156}Gd, ^{158}Gd and ^{160}Gd do not significantly ruin the performance of the burnable poison. A total abundance of 50–60% of the odd isotopes is adequate for use as burnable poison.

Gadolinium has the ground state configuration of $[Xe]4f^{7}5d6s^{2}$ having extremely complex level structure and has innumerable transitions available for resonance ionisation studies. In the process of enriching the isotope of interest, it is important to identify the most efficient atomic transition which yields large isotopic selectivity. Balling and Wright [3] have proposed a method for isotope selective excitation of non-zero nuclear spin isotopes using polarization selection rules. Guyadec et al. [4] have used multistep photoionization scheme with polarized lasers, for isotope selective excitation of odd isotopes of gadolinium in a magnetic field where a large degree of enrichment has been obtained. Utilization of such photoionization schemes for Atomic Vapor Laser Isotope Separation (AVLIS) is not viable because they involve magnetic fields which increases the complexity of the experimental geometry.

Santala et al. [2] have recently carried out double resonance ionization experiments for isotope selective

* Corresponding author. Tel.: +91-40 712 3546; fax: +91-40 712 5463; e-mail: sankari@cccm1.ernet.in.

0022-3115/99/$ – see front matter
PII: S0022-3115(98)00480-2

ionisation of odd gadolinium isotopes. They have obtained enrichment of about 45–70% for the odd isotopes of gadolinium. The photoionization scheme used by them involves excitation transitions in the UV region. This necessitates the use of a frequency doubler in the photoionization scheme resulting in poor photon economy. For industrial scale enrichment, the photoionization scheme must involve transitions that can be produced by high repetition rate lasers such as copper vapor laser (CVL) pumped dye lasers for improved duty cycles.

We have recently used spectral simulation method for studying isotope selective excitations of low abundant ^{138}La isotope using diode laser initiated resonance ionisation mass spectrometry [5], Gd isotopes for narrowband laser excitation [6] and isotope selective enrichment of ^{168}Yb isotopes using broadband lasers [7]. A good agreement in the computed and experimental isotopic selectivities was obtained for lithium [8] and lanthanum [5] isotopes. In the present work, we have examined the possibility of using gadolinium transitions in the 560–590 nm region (rhodamine 6G dye region) originating from $^{9}D^{\circ}_{2-6}$ ground states for selective excitation of ^{155}Gd and ^{157}Gd isotopes. The present photoionization scheme has the following merits.

(1) The first excitation step which is a resonant step, involves transitions which can be pumped by rhodamine 6G dye. Since rhodamine 6G dye can be pumped with large conversion efficiencies using CVL as pump laser, duty cycle of the process can be improved enabling industrial scaling of the process. In the photoionization schemes used by Santala et al. [2], the first resonant excitation step involves transitions which lie in the UV region. Since this requires the utilization of a frequency doubler for the generation of UV light, the resultant photon economy is rather poor.

(2) Since the present photoionization scheme does not require frequency doubler for the first excitation step, it results in better photon economy compared to the photoionization schemes used earlier [2].

(3) The photoionization scheme has simple experimental geometry.

However such simple photoionization schemes must result in adequate selectivities. In the present work, we have considered few transitions in the rhodamine 6G region to evaluate their efficacy for selective excitation of odd gadolinium isotopes. In order to have an effective comparison with the results reported earlier [2], we have used only one resonant excitation step. The atoms pumped into the first excited state are ionized (non-resonantly) using UV laser.

2. Principle

In laser spectroscopic experiments, isotope selective excitation is carried out using isotope shift of the selected optical transition. Isotopic selectivity (S) is defined by the ability to detect low abundant rare isotope in the presence of the other high abundant isotopes. In an optical transition the maximum isotopic selectivity that can be achieved is limited by the natural Lorentzian line shape [9].

$$\text{Selectivity } S = \left[\frac{2\Delta v}{\Gamma_{\text{nat}}}\right]^2, \tag{1}$$

where Γ_{nat} is the homogeneous natural linewidth and Δv the isotope shift of the transition.

The additional inhomogeneous broadening Γ_{inh} from Doppler distributions or finite laser linewidths further reduces the optical isotopic selectivity [10] by a factor of $\Gamma_{\text{nat}}/\left(\sqrt{\pi \ln 2}\Gamma_{\text{inh}}\right)$.

In this approach, the atomic line profile (assuming a Lorentzian profile) is generated first taking into account the appropriate abundances, isotope shifts of the constituent isotopes and hyperfine structure of odd isotopes.

The Lorentzian line profile can be expressed as

$$L(\omega) = \frac{2}{\pi\Delta\omega 0}\left[\frac{1}{1+\left\{\frac{2(\omega 0-\omega)}{\Delta\omega 0}\right\}^2}\right], \tag{2}$$

where ω_0 is the resonance frequency of the transition, $\Delta\omega_0$ the full width at half maximum (FWHM) of the transition and $L(\omega)$ the intensity at the frequency ω.

The relative intensities of the transition between HFS components of the ground and excited states can be expressed as [11]

$$I(F-F') = (2F+1)(2F'+1)\begin{Bmatrix} J & F & I \\ F' & J' & 1 \end{Bmatrix}^2,$$

where F, J are the total and electronic angular momentum of the ground and excited states and I is the nuclear spin of the isotope under consideration. The prime denotes the excited states.

The relative intensity for the various transitions has been computed using Clebsch–Gordon algebra for the selection rules $\Delta J = 0, \pm 1$ and $\Delta F = 0, \pm 1$. The energy of the HFS component is given by the Casimir formula,

$$W_{\text{F}} = W_{\text{J}-} + \frac{C}{2}A + \frac{3C(C+1) - 4I(I+1)J(J+1)}{8I(2I-1)J(2J-1)}B,$$

where $C = F(F+1) - I(I+1) - J(J+1)$

In the present simulation approach, the relative intensities of the HFS components for the odd isotopes are computed using the ground and excited state electronic angular momentum (J), total angular momentum (F)

and the nuclear spin of the isotope (I). The nuclear spin of both the odd isotopes is 3/2. The relative frequency positions are computed using the Casimir formula substituting the hyperfine structure constants reported earlier [11]. The excitation spectrum is generated from the resultant atomic line profile by using the appropriate laser linewidth. The laser line profile is assumed to be Gaussian.

Isotopic selectivity for a transition is defined as the ratio of the intensity of the isotope of interest at its resonance to the intensity of the interfering isotope at the resonance frequency of the isotope of interest.

$$\text{Isotopic selectivity } S(\omega) = \frac{I_{\mathrm{M1}}(\omega)}{I_{\mathrm{M2}}(\omega)}, \tag{3}$$

where I_{M1} is the intensity of the M1 isotope at the resonance frequency (ω) and I_{M2} the intensity of the interfering M2 isotope at the resonance frequency (ω) of M1.

In a case where more than two isotopes are involved the isotopic selectivity is defined as

$$\text{Isotopic selectivity } S(\omega) = \frac{I_{\mathrm{M1}}(\omega)}{I_{\mathrm{all}}(\omega)}, \tag{4}$$

where I_{all} is the intensity of all the isotopes at resonance frequency (ω) of the isotope M1. The selectivity of the overall photoionization scheme under consideration can be given by the expression

$$S = S_{\mathrm{exc}} S_{\mathrm{ion}}, \tag{5}$$

where S_{exc} is the selectivity of the excitation transition and S_{ion} the selectivity of the ionization process. Since the ionization process (being non-resonant) does not yield any additional selectivity, the overall selectivity of the process can be expressed as

$$S = S_{\mathrm{exc}}. \tag{6}$$

The abundances of the constituent isotopes can be calculated using the computed isotopic selectivity values. The method has the following merits.

(a) The atomic lines are predominantly Gaussian at peaks and Lorentzian at wings. Since the isotopic selectivities are limited by wing absorption of the atomic lines, it is adequate to consider the atomic profile to be Lorentzian.

(b) In case the laser line profile is assumed Lorentzian, then it may lead to unphysical results. This necessitates the introduction of a cutoff parameter (β) in order to obtain realistic values [12]. Assuming the laser line profile to be Gaussian eliminates the need for the introduction of a cutoff parameter for computation. However, most reliable results can be obtained only when computations are done using the laser line shape as determined during individual experiments.

(c) The effect of hyperfine structure of the odd isotopes, abundance of the constituent isotopes, laser linewidth and the laser line shape is incorporated in the computation.

In isotope selective excitation processes, increase in laser intensity deteriorates the overall selectivity due to Stark broadening, power broadening and nonselective wing absorptions. Power broadening is proportional to $I^{n/2}$ (where n is the number of photons involved in the n-photon bound–bound transition and I the intensity of the laser radiation) whereas ac Stark shift is proportional to I. The effects of power broadening and ac Stark shift can be minimized using optimum laser intensities. Since the isotope selectivity calculations do not include power broadening and Stark broadening effects, operating in the optimum laser intensity region should result in theoretically computed abundances.

3. Experimental

The experimental setup (Fig. 1) used for the present investigations constitutes an XeCl excimer laser (Lumonics PM-848, 300 mJ, 200 Hz, 15 ns) pumping two grazing incidence dye lasers (Lumonics HD-540, linewidth ~1200 MHz) with rhodamine-6G dye. A frequency doubler (Lumonics HT-1000, KDP) was used with one of the dye lasers to obtain UV output for the ionization step. Calibration of the dye laser was done by recording the optogalvanic emission spectrum of the Ne lines in a commercial Au / Ne hollow cathode lamp (M/s. Cathodeon, UK) filled with neon buffer gas.

A water cooled resistively heated atomic beam furnace with graphite crucible atomizer, similar to that used by Bekov and Letokhov [13] was used for generating the atomic beam. Gadolinium powder (Leico, >99.99% pure) was loaded in the crucible and heated to about ~1500°C by applying a current of ~200 A using a power supply (20VAC, 300 A). The power supply was operated in constant current mode. A single color optical pyrometer was used for calibration of the furnace temperature.

Out of the 20 transitions for which isotopic selectivities were computed, 11 transitions have been selected in the region where good conversion efficiency can be obtained for rhodamine-6G dye. The excitation laser (λ_1) was tuned to the resonance of one of the transitions. The second dye laser was frequency doubled using the frequency doubler and tuned to 292 nm (λ_2) for ionization. The pulse energy was sufficiently reduced to prevent saturation broadening and multiphoton ionization of the atoms. The ion signal disappeared when any of the two lasers was blocked ensuring multistep photoionization rather than multiphoton ionization. The typical pulse energies used in the excitation step were ~5 μJ and about 100 μJ in the ionization step. The linewidth of the excitation laser is 1200 MHz. The laser beams interact with the atomic beam orthogonally. The beam diameter

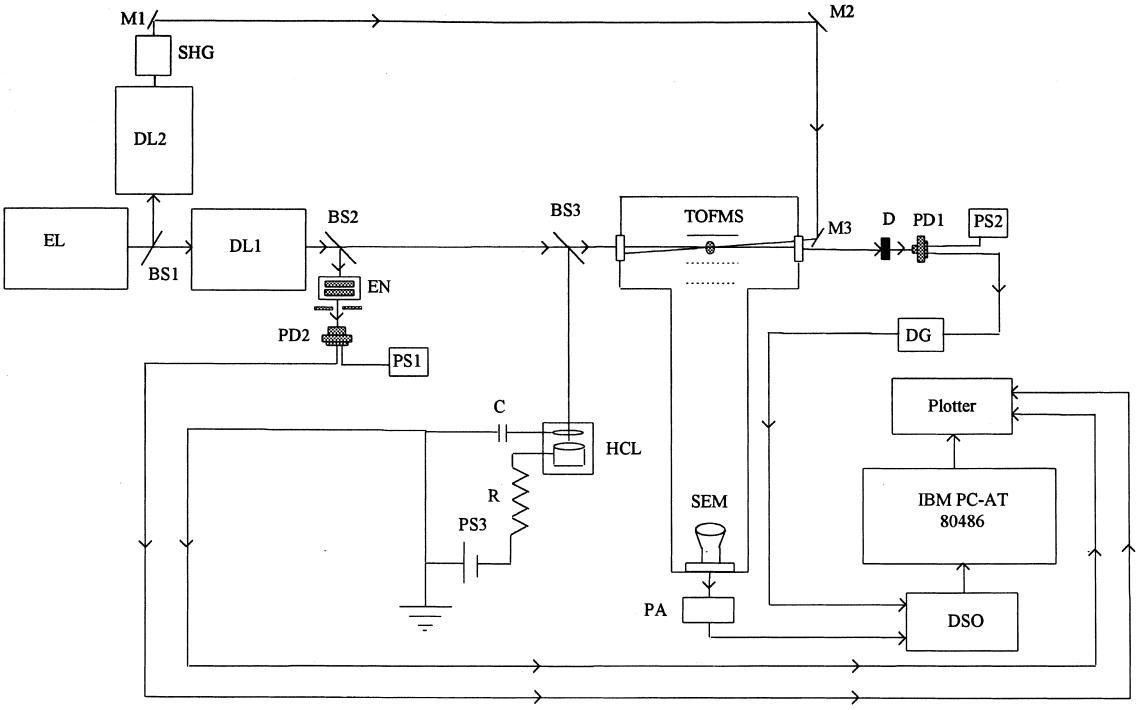

Fig. 1. Schematic of the experimental setup. BS – Beam Splitter, C – Capacitor, D – Diffusor, DG – Delay Generator, DL – Dye Laser, DSO – Digital Storage Oscilloscope, EL – Excimer Laser, EN – 7.5 GHz Air Spaced Etalon, HCL – Hollow Cathode Lamp, M – Mirror, PA – Preamplifier, PD – Photodiode, PS – Power Supply, R – Current Limiting Resistor, SEM – Secondary Electron Multiplier, SHG – Frequency Doubler, TOFMS – Time-of-flight Mass Spectrometer.

was about ~1.5 mm at the laser beam – atomic beam interaction zone. At the furnace operating temperatures of ~1500°C, the residual Doppler width of the atomic beam as a result of collimation, is 800 MHz.

An indigenous Wiley – McLaren type time-of-flight (TOF) mass spectrometer with a 120 cm long field free region and a resolution (T/2ΔT) of 400 was used for recording the TOF spectrum of the photoions. The photoions were extracted into the mass spectrometer using two-stage acceleration. The total acceleration voltage applied was 2500 V. A two-stage DC-300 MHz preamplifier (Stanford Research Systems, SR240) with single stage gain of 5 was used to amplify the output of a secondary electron multiplier (Phillips, X959BL). The amplified signal was fed to a digital storage oscilloscope (Tektronix TDS- 350, 200 MHz, 1 GS/s 2% vertical accuracy) and stored. The data were averaged for 256 pulses and transferred to a computer for further analysis.

4. Resonance ionization of gadolinium

Gadolinium falls in the lanthanide group of elements having a ground state configuration of $[Xe]4f^7 5d6s^2$ in the valence shell. It has five low lying odd parity metastable states having energies 0.0 cm^{-1} ($^9D°_2$), 215.124 cm^{-1} ($^9D°_3$), 532.977 cm^{-1} ($^9D°_4$), 999.121 cm^{-1} ($^9D°_5$) and 1719.087 cm^{-1} ($^9D°_6$). At an operating temperature of ~1500°C of the atom generation source, the population in any of these states can be in the range of about 12–25% and the total population in these states is ~99%. The $^{11}F°_{2-8}$ odd parity metastable states are in the energy range of 6300–8500 cm^{-1} and have a population of $\leqslant 1\%$. For efficient isotope selective excitation / ionization of gadolinium, the excitation transition in the photoionization scheme must involve the highly populated $^9D°_{2-6}$ states.

Niki et al. [11] have measured the hyperfine structure of the odd isotopes for the transitions lying in the tuning range of rhodamine-6G dye. The magnetic dipole (A) and electric quadrupole (B) constants were determined using laser induced fluorescence experiments. The even ^{154}Gd and ^{156}Gd isotopes effectively overlap with the spectrum of odd gadolinium isotopes because of the relatively small isotope shifts and large hyperfine splitting [11,14–16] of the odd isotopes, thus making isotope selective excitation of odd gadolinium isotopes a difficult task. The dilution of oscillator strength among the hyperfine components for odd isotopes further reduces the isotopic selectivity. We have considered 20 transitions

which originate from the odd parity $^9D^\circ_{2-6}$ metastable states that fall within the tuning range of rhodamine-6G dye. The atoms are ionized from these excited states by absorbing another UV photon (Fig. 2). The efficacy of such photoionization schemes depends on the overall enrichment that can be obtained.

5. Results and discussion

Isotopic selectivities have been computed for all the 20 transitions considered. The excitation spectra have been simulated for all these transitions taking into account the appropriate abundances of the constituent

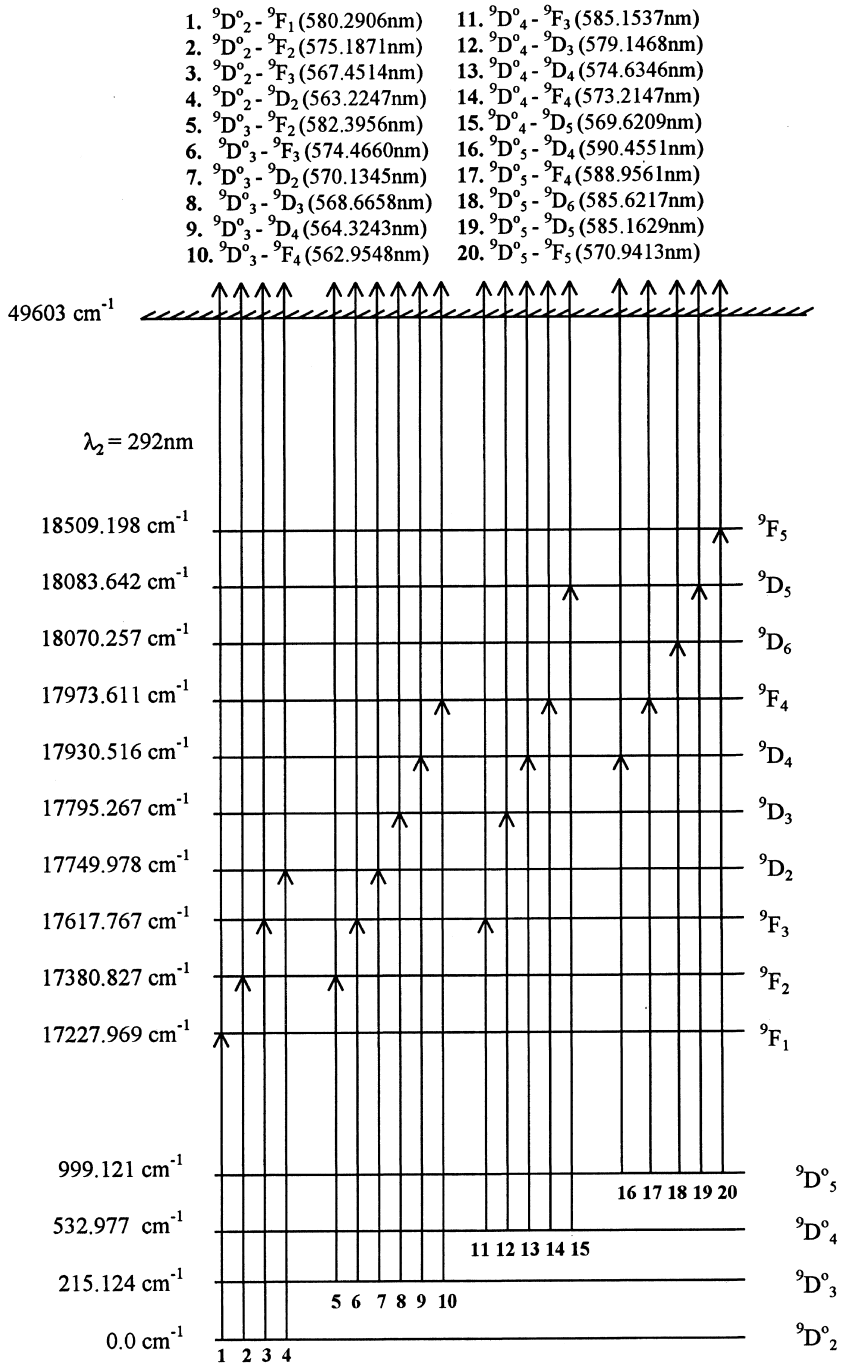

Fig. 2. Schematic of the photoionization schemes used for isotope selective excitation of odd gadolinium isotopes.

isotopes and hyperfine structure of odd isotopes. The isotopic selectivity of the isotope of interest is dependent on the residual Doppler width (Doppler width along the laser axis) of the atomic beam and the linewidth of the excitation laser. Isotopic selectivity calculations have been carried out for various laser linewidths and residual Doppler widths in the range of 50–1200 MHz. Maximum overlap of the atomic and laser profile is ensured when the residual Doppler width of the atomic beam is of the order of linewidth of the excitation laser. Hence, in this set of calculations, residual Doppler width of the atomic beam is considered same as the linewidth of the excitation laser. A typical plot of the isotopic abundances calculated as a function of laser linewidth is plotted in Fig. 3. The content of ^{155}Gd and ^{157}Gd isotopes can be raised to >90% from the natural abundance when a narrowband laser with a linewidth of 50 MHz is used in the excitation scheme. With an increase in the laser linewidth, the isotopic abundance of the odd isotope reduces as a result of decrease in the isotopic selectivity. Isotopic selectivities, isotopic abundances and microscopic capture cross-section (σ) of the isotopic mixture for all the 20 transitions were computed for a laser linewidth of 1200 MHz. The overall degree of enrichment is comparable for all the transitions considered.

The TOF spectra were recorded for all the 11 transitions, by tuning the excitation laser (λ_1) to the appropriate wavelength and the resonance position of ^{160}Gd isotope was identified using gated detection with a boxcar averager. The resonance frequency of ^{160}Gd was chosen as the reference position. The laser was then detuned to 1, 2, 3, 4 and 5 GHz (towards lower wavelength) relative to ^{160}Gd and the TOF mass spectra were recorded. A simulated excitation spectra for the $^9D°_5$–$^9D_4$ (590.4551 nm) transition for a laser linewidth of 1200 MHz and a residual Doppler width of 800 MHz and for a laser linewidth of 50 MHz and a residual Doppler width of 50 MHz are plotted in Fig. 4(a). TOF spectra were recorded for different detuning wavelengths within the resonance structure of the $^9D°_5$–$^9D_4$ (590.4551 nm) transition as shown by the vertical dashed lines in Fig. 4(a) (Fig. 4(b)–(g)). When the laser is gradually detuned from ^{160}Gd to shorter wavelengths (Fig. 4(b)–(g)), the signal due to heavier isotopes decreases and the lighter isotopes start appearing. At some intermediate detuning (~3000 MHz) from the resonance position of ^{160}Gd isotope, the fraction of odd isotopes in the

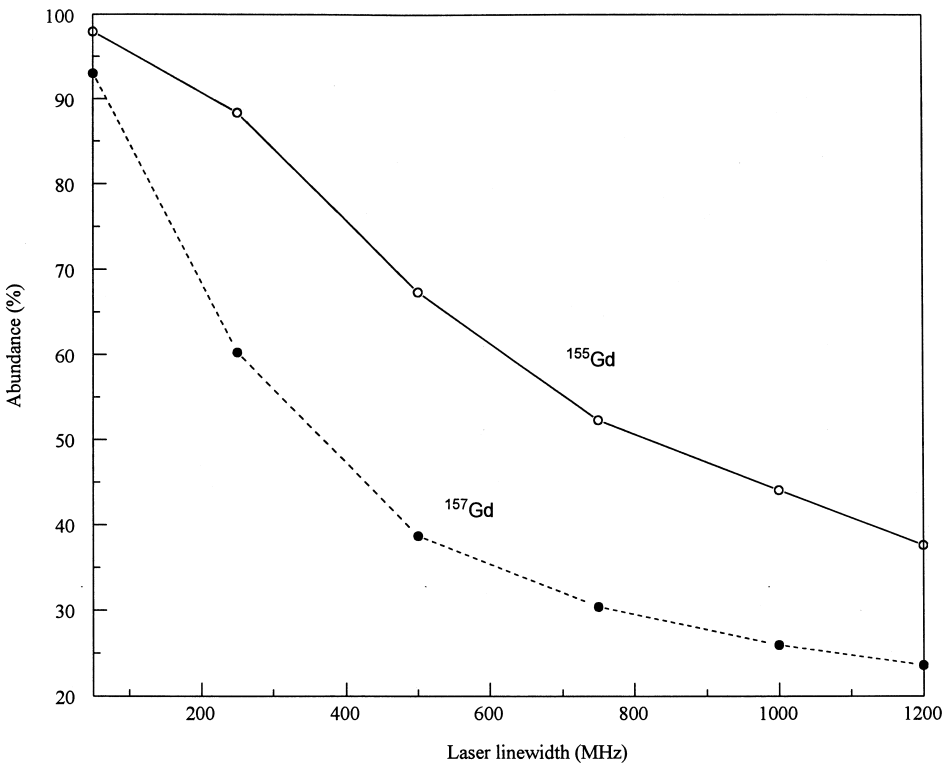

Fig. 3. The dependence of isotopic abundance of ^{155}Gd (solid line) and ^{157}Gd (dashed line) as a function of laser linewidth for the $^9D°_5$–$^9F_4$ (588.9561 nm) transition. The residual Doppler width of the atomic beam is considered to be same as the laser linewidth.

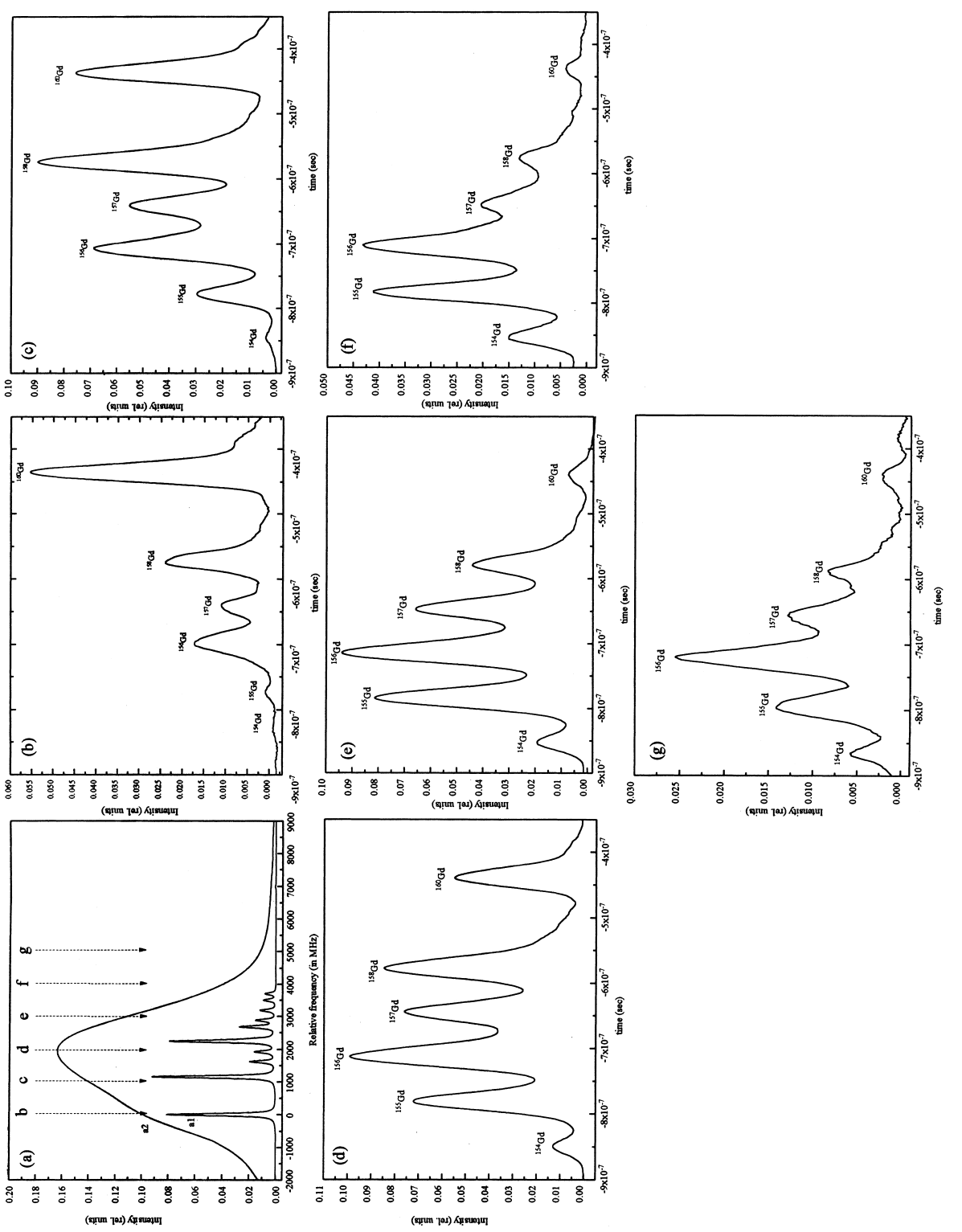
(a)
(b)
(c)
(d)
(e)
(f)
(g)
a1
a2
b c d e f g
Intensity (rel. units)
Relative frequency (in MHz)
time (sec)
154Gd
155Gd
156Gd
157Gd
158Gd
160Gd

photoion signal is the largest. The relative compositions of the isotopic mixtures have been determined by deconvoluting the TOF spectrum. The exact isotopic fractions observed are not sensitive to the peak shape used in the fitting because, the resolution of the TOF mass spectrometer is fairly high ($M/\Delta M = 400$). Tuning the dye laser to the computed maxima of ^{155}Gd isotope (i.e., the detuned position where isotopic selectivity of ^{155}Gd isotope is largest) resulted in 38% of ^{155}Gd isotope. Similarly when the dye laser was tuned to the maxima of ^{157}Gd isotope the abundance of ^{157}Gd isotope was 24%.

5.1. Thermal neutron absorption properties of the enriched isotopic mixture

Among the odd gadolinium isotopes, as mentioned earlier, ^{157}Gd has large neutron absorption cross-section and it is desirable to achieve enrichment of this isotope. Even though the linewidth of the excitation laser limits the overall enrichment of the odd isotopes using this excitation scheme, tuning the dye laser to an appropriate position within the resonance structure results in an optimum concentration of ^{155}Gd and ^{157}Gd isotopes. In order to find such optimum position, computation of isotopic selectivities has been carried out considering appropriate initial parameters such as linewidth of the excitation laser, residual Doppler width, isotope shifts and hyperfine structure of the odd isotopes. The relative isotopic abundances and the microscopic capture cross-section of the isotopic mixture as a function of laser detuning have been computed using the isotopic selectivity values (Fig. 5). As seen from Fig. 5(c), when the dye laser is tuned to the resonance of ^{155}Gd isotope for the $^9D°_5$–$^9D_4$ (590.4551 nm) transition, the total microscopic capture cross-section of the isotopic mixture amounts to 62,100 b. Similarly when the excitation laser is tuned to the resonance of ^{157}Gd isotope, the total microscopic capture cross-section of the isotopic mixture is 69,200 b. Since the theoretically expected limit of the total microscopic capture cross-section of the isotopic mixture is 71,500 b, both these frequency positions do not lead to an optimum isotopic composition. Thus, detuning the laser in between the resonance positions of ^{155}Gd and ^{157}Gd isotopes results in optimum isotopic composition and microscopic capture cross-section of the isotopic mixture. The isotopic abundances measured for various detunings of the dye laser was in agreement with the theoretical results (Fig. 5(b)).

◀ Fig. 4. (a) Simulated excitation spectra for laser linewidths of 50 MHz (a1) and 1200 MHz (a2). (b)–(g) TOF spectra recorded for various detunings within the resonance structure of the $^9D°_5$–$^9D_4$ (590.4551 nm) transition. The vertical lines in Fig. 4(a) indicate the detuned positions in the transition. The spectra were recorded with a trigger delay of 21.4 μs after the laser pulse and 256 averages.

TOF spectra were recorded for all the 11 transitions, by tuning the excitation laser to the computed optimum frequency position and the results obtained are tabulated in Table 1. As seen from Table 1, the total isotopic composition of ^{155}Gd and ^{157}Gd isotopes can be increased to ~50% from their natural abundance of 30% using any of these transitions. Apart from obtaining optimum abundance of the odd isotopes, it is also important to find the relative abundances of other even isotopes particularly ^{152}Gd and ^{154}Gd, as these isotopes increase the residual neutron absorption in the irradiated fuel. When the laser was tuned to the optimum frequency position, the abundance of ^{154}Gd isotope was found to be about 1% for all the 11 transitions, whereas the abundance of ^{152}Gd isotope was not within the detectable limits of the ion detection system (minimum detectable limit ~0.05%). However, from theoretical calculations the abundance of ^{152}Gd isotope was estimated to be <0.004% for all the transitions considered. This ensures adequate depletion of ^{152}Gd isotope in the resultant isotopic mixture. The abundances of the gadolinium isotopes computed for the optimum frequency position for the $^9D°_5$–$^9F_4$ (588.9561 nm) transition and the experimentally obtained abundances are plotted in Fig. 6. The thermal neutron absorption property of the resultant isotopic mixture has been analyzed analytically [2] for using it as a burnable poison in reactors (Table 2). The enriched gadolinium has 50% larger microscopic capture cross-section as compared to natural gadolinium. More significantly, the enriched isotopic mixture is depleted in ^{152}Gd and ^{154}Gd isotopes which reduces the residual absorption of the irradiated fuel by 70%. The increase in the microscopic capture cross-section is adequate to use it as an efficient burnable poison.

The present calculations ignore the longitudinal mode structure of the excitation laser, which could result in the pulse-to-pulse variation in the isotope yield. Such variation is not expected to reduce the degree of enrichment substantially as evident from the experimental results. Hence, utilization of single mode dye lasers for such enrichments appears to be needless. However, utilization of such photoionization schemes necessitates the long term wavelength stabilization of the dye lasers. Even though, problems related to the industrial use of these photoionization schemes are not part of the present study, the feasibility of enrichment of ^{155}Gd and ^{157}Gd isotopes with relatively broadband lasers is established. The degree of enrichment though partial, is adequate for all practical purposes.

6. Conclusion

The feasibility of isotope enrichment of ^{155}Gd and ^{157}Gd isotopes using relatively broadband lasers within

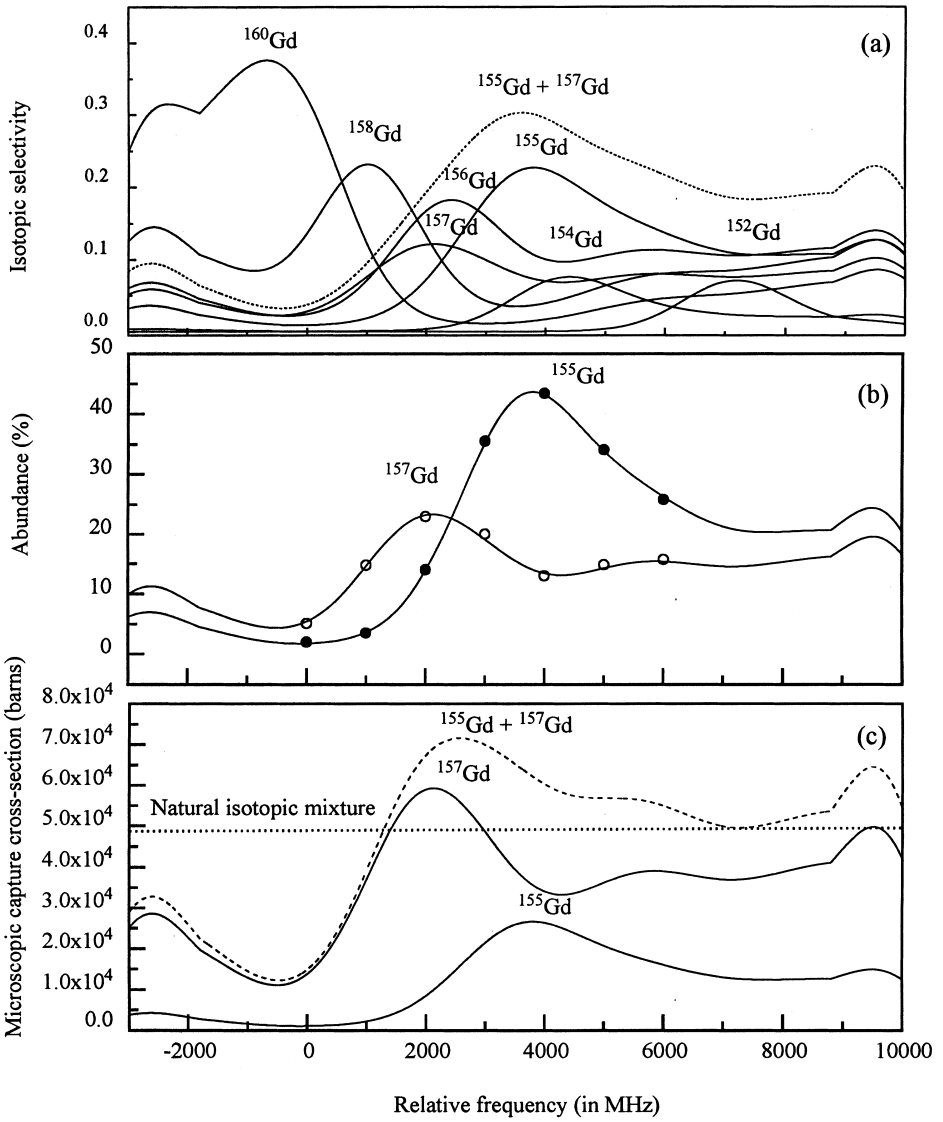

Fig. 5. Computed isotopic selectivities (a), abundances (b) and microscopic capture cross-sections (c) of gadolinium isotopes as a function of laser detuning for the $^{9}D^{\circ}_{5}$–$^{9}D_{4}$ (590.4551 nm) transition. The experimentally determined abundances for ^{155}Gd (solid circle) and ^{157}Gd (open circle) for various detunings are also plotted in (b).

the tuning range of rhodamine-6G dye has been studied. A new set of photoionization schemes with improved photon economy and less experimental complexity have been proposed for industrial scale enrichment of these isotopes. The degree of enrichment for the present photoionization scheme is adequate for using the enriched mixture as an efficient burnable poison.

The abundances of the constituent isotopes as a function of the laser frequency (within the resonance structure) have been computed using spectral simulation approach, incorporating the laser parameters (such as linewidth) and spectroscopic parameters (such as isotope shifts and hyperfine structure). The isotopic abundances computed for various transitions were found to be in good agreement with the experimental results. This approach has been used for calculation of isotopic selectivities in order to identify the most efficient atomic transitions for isotope enrichment and to focus experimental effort on these transitions.

Alternatively, it may be worthwhile to attempt isotope selective separation of ^{152}Gd and ^{154}Gd from natural gadolinium since these isotopes have deleterious effects on the performance of gadolinium as burnable poison. Viability of such methods critically depend on the extent of sacrifice in the experimental simplicity in order to obtain higher degree of enrichment.

Table 1
Comparison of experimental and theoretical isotopic abundances of ^{155}Gd and ^{157}Gd isotopes obtained for the various transitions when the dye laser is tuned to the computed optimum frequency position

Transition	% abundance of ^{155}Gd		% abundance of ^{157}Gd		Microscopic capture cross-section (σ) of the isotopic mixture	
	Theoretical	Experimental	Theoretical	Experimental	Theoretical	Experimental
$^9D°_3$–$^9D_2$ (570.1345 nm)	30.6	32.7	18.7	19.2	66 100	68 700
$^9D°_4$–$^9D_4$ (574.6346 nm)	29.2	30.3	18.1	20.6	63 700	70 800
$^9D°_2$–$^9F_2$ (575.1871 nm)	22.7	24.7	20.2	22.9	65 100	73 200
$^9D°_4$–$^9D_3$ (579.1368 nm)	30.6	29.1	18.1	20.1	64 600	68 800
$^9D°_2$–$^9F_1$ (580.2906 nm)	–	22.7	–	20.8	–	66 700
$^9D°_3$–$^9F_2$ (582.3956 nm)	23.0	23.6	19.8	23.0	64 300	72 800
$^9D°_4$–$^9F_3$ (585.1537 nm)	22.7	19.7	22.3	23.9	70 500	72 700
$^9D°_5$–$^9D_5$ (585.1629 nm)	41.5	29.7	19.1	21.0	73 800	71 400
$^9D°_5$–$^9D_6$ (585.6217 nm)	38.7	28.6	19.1	21.6	72 100	72 300
$^9D°_5$–$^9F_4$ (588.9561 nm)	21.5	20.0	24.3	24.3	74 800	73 900
$^9D°_5$–$^9D_4$ (590.4551 nm)	25.8	24.1	20.9	22.0	68 800	70 600

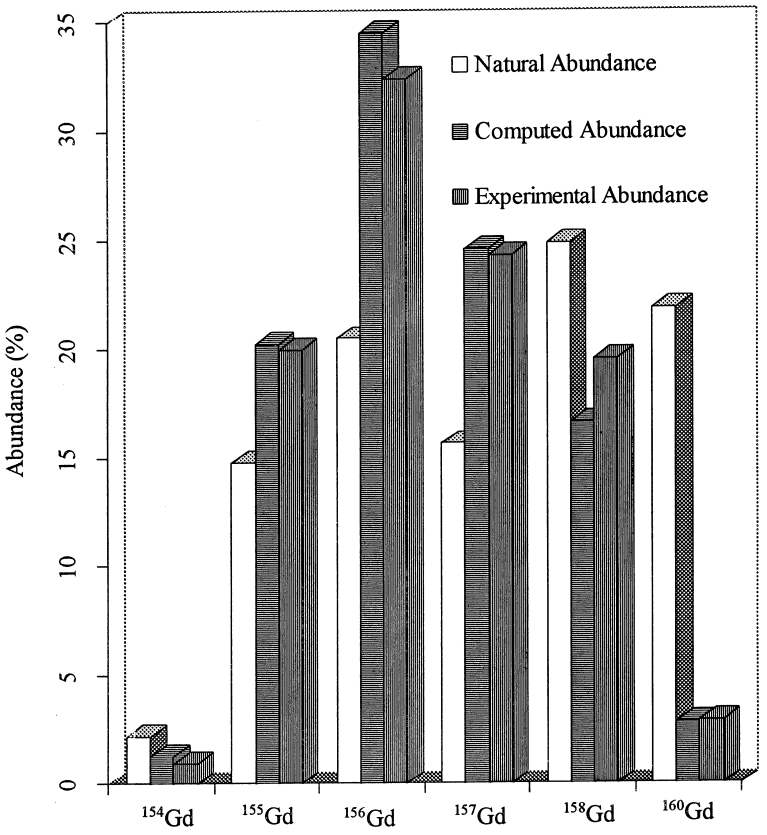

Fig. 6. The experimentally obtained and theoretically computed isotopic abundances using a laser with a linewidth of 1200 MHz for the $^9D°_5$–$^9F_4$ (588.9561 nm) transition. The dye laser was tuned to obtain the optimum isotopic composition of the odd isotopes.

Table 2
Thermal neutron absorption properties of natural and enriched mixtures of gadolinium for the $^9D°_5$–$^9F_4$ (588.9561 nm) transition

Isotope	$\sigma_{\gamma,n}$	Nat. isotopic mixture (unused)		Nat. isotopic mixture (used)		Enriched isotopic mixture (unused)		Enriched isotopic mixture (used)	
		Abun	σ	Abun	σ	Abun	σ	Abun	σ
^{152}Gd	735	0.2	1.47	0.2	1.47	0	0	0	0
^{153}Gd	36 000	0	0	0	1.47	0	0	0	0
^{154}Gd	85	2.15	1.83	2.15	1.83	1.0	0.85	1.0	0.85
^{155}Gd	60 900	14.73	8970.6	0.0	1.83	20.0	12 180.0	0	0
^{156}Gd	1.5	20.47	0.3	35.2	0.53	32.4	0.49	52.4	0.79
^{157}Gd	254 000	15.68	39 827.2	0.0	0.53	24.3	61 722	0	0
^{158}Gd	2.2	24.87	0.6	40.55	0.89	19.5	0.43	43.8	0.96
^{160}Gd	0.8	21.90	0.2	21.9	0.17	3.0	0.02	3.0	0.02
Total		100	48 800		8.72	100	73 900		2.62

$\sigma_{\gamma,n}$ – Thermal neutron absorption cross-section.
σ – Microscopic capture cross-section.

Even though the selectivities of the photoionization schemes used in the present work are adequate for isotope selective separation of odd gadolinium isotopes, the selectivities could be improved further using mutlistep photoionization schemes involving autoionization states. However it requires large amount of experimental and theoretical work to identify transitions which have large isotopic selectivities. At present we are working on such multistep photoionization schemes.

References

[1] Review of fuel developments for Water Cooled Nuclear Power Reactors, IAEA Vienna, Technical Reports Series No. 299 (1989).
[2] M.I.K. Santala, A.S. Davittila, H.M. Lauranto, R.R.E. Salomaa, Appl. Phys. B 64 (1997) 334.
[3] L.C. Balling, J.J. Wright, Appl. Phys. Lett. 29 (1976) 411.
[4] E. Le Guyadec, J. Ravoire, R. Botter, F. Lambert, A. Petit, Opt. Commun. 76 (1990) 34.
[5] M. Sankari, M.V. Suryanarayana, Spectrochim. Acta B 52 (1997) 735.
[6] M.V. Suryanarayana, M. Sankari, Z. Phys. D 39 (1997) 35.
[7] M. Sankari, M.V. Suryanarayana, J. Phys. B 31 (1998) 261.
[8] M.V. Suryanarayana, M. Sankari, Int. J. Mass Spectrom. Ion Proc. 173 (1998) 177.
[9] Y.A. Kudriavtsev, V.S. Letokhov, Appl. Phys. B 29 (1982) 219.
[10] L. Monz, R. Hohmann, H.-J. Kluge, S. Kunze, J. Lantzsch, E.W. Otten, G. Passler, P. Senne, J. Stenner, K. Stratmann, K. Wendt, K. Zimmer, Spectrochim. Acta B 48 (1993) 1655.
[11] H. Niki, T. Miyamoto, Y. Izawa, S. Nakai, C. Yamanaka, Opt. Commun. 70 (1989) 16.
[12] P. Zoller, P. Lambropoulos, Phys. Rev. B 12 (1979) L547.
[13] G.I. Bekov, V.S. Letokhov, Appl. Phys. B 30 (1983) 161.
[14] H.-D. Kronfeldt, G. Klemz, S. Kroger, J.-F. Wyart, Phys. Rev. A 48 (1993) 4500.
[15] W.G. Jin, H. Sakata, M. Wakasugi, T. Horiguchi, Y. Yoshizawa, Phys. Rev. A 42 (1990) 1416.
[16] S.B. Dutta, A.G. Martin, W.F. Rogers, D.L. Clark, Phys. Rev. C 42 (1990) 1911.